



Universiteit  
Leiden  
The Netherlands

## **Ln(III) complexes as potential phosphors for white LEDs**

Akerboom, S.

### **Citation**

Akerboom, S. (2013, October 29). *Ln(III) complexes as potential phosphors for white LEDs*. Retrieved from <https://hdl.handle.net/1887/22054>

Version: Not Applicable (or Unknown)

License: [Leiden University Non-exclusive license](#)

Downloaded from: <https://hdl.handle.net/1887/22054>

**Note:** To cite this publication please use the final published version (if applicable).

Cover Page



Universiteit Leiden



The handle <http://hdl.handle.net/1887/22054> holds various files of this Leiden University dissertation.

**Author:** Akerboom, Sebastiaan

**Title:** Ln(III) complexes as potential phosphors for white LEDs

**Issue Date:** 2013-10-29

# 4 Phenol-type ligands as sensitizers

*Eight new complexes of europium(III) and terbium(III) using 2-(4,5-dihydro-1,3-oxazol-2-yl)phenol (HL1) and 2-(4,5-dihydro-1,3-thiazol-2-yl)phenol (HL2) as ligands have been prepared in yields ranging between 74 and 100%. Depending on the synthetic strategy employed, ligand-to-metal ratios of 1:3 and 1:4 can be achieved, giving rise to compounds with the formulae  $[Ln_2(L)_6]$  and  $NR_4[Ln(L)_4]$ , Ln = Eu, Tb and R = ethyl, n-butyl. An attempt at recrystallisation of the complexes from dmsO resulted in the formation of an octanuclear complex held tightly together by carbonate ions that have been formed from  $CO_2$  captured from the atmosphere. Those compounds are described by the general formula  $[Na_2(Ln(L1)_3)_2(CO_3)(dmsO)_2]_2$ . Of five compounds, the crystal structures have been determined, all showing a bidentate mode of binding of the ligand via the phenolate oxygen and the nitrogen atom of the five-membered ring. The compounds  $[Tb_2(L1)_6]$ ,  $NBu_4[Tb(L1)_4]$ ,  $[Tb_2(L2)_6]$  and  $[Na_2(Tb(L1)_3)_2(CO_3)(dmsO)_2]_2$  show bright luminescence characteristic for the Tb(III) ion upon excitation with near-UV radiation, with quantum yields ranging from 16% to 79%. Strong emission typical for the Eu(III) ion is observed for  $NBu_4[Eu(L1)_4]$  and  $NEt_4[Eu(L2)_4]$  with quantum yields of 43% and 20%, respectively. The other compounds are only very weakly luminescent.*

(This Chapter will be published: S. Akerboom, E. Tom Hazenberg, I. Schrader, S.F. Verbeek, I. Mutikainen, W. T. Fu, E. Bouwman, manuscript in preparation)

## 4.1 Introduction

In Chapter 1 of this thesis, it is discussed how highly energy efficient LED-based Solid State Lighting (SSL) sources have the potential to replace the conventional light bulbs [1]. This in turn would save large amounts of energy and reduce CO<sub>2</sub> emissions [2]. New phosphor materials that can efficiently convert nUV or blue radiation into visible light are required for the development of highly efficient SSLs [3-6]. Although phosphor materials are widely used in today's lighting and display technologies, they have been designed for high energy excitation sources and cannot be efficiently excited in the nUV of blue spectral region [7]. Complexes of the trivalent lanthanoid ions are attractive candidate phosphor materials because of their broad, ligand centered excitation bands and line like emission spectra characteristic of the lanthanoid ion [8]. Ligands that are currently known to efficiently sensitize luminescence of the lanthanoids include beta-diketonates, aromatic carboxylates, salicylates and polycyclic heteroaromatic ligands such as 1,10-phenanthroline and 2,2'-bipyridine [9-16]. Previous work on the use of benzoxazole and benzothiazole substituted pyridine-2-carboxylate as a ligand to the lanthanoids has demonstrated these ligands to be highly capable of sensitizing lanthanoid-centered luminescence, in particular that of Eu(III) [17]. Salicylate-type ligands are found to be highly efficient at sensitizing luminescence by the Tb(III) ion, while they generally fail to excite Eu(III) luminescence [14, 18]. In view of this, oxazoline and thiazoline substituted phenols seem attractive antenna ligands for enhancing luminescence of Eu(III) and Tb(III) ions. This Chapter reports on the synthesis, characterization, structure and photophysical properties of a family of Eu(III) and Tb(III) complexes with 2-(4,5-dihydro-1,3-oxazol-2-yl) phenol (**HL1**) and 2-(4,5-dihydro-1,3-thiazol-2-yl)phenol (**HL2**) as ligands. The compounds discussed are shown in Figure 4.1.

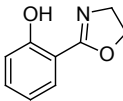
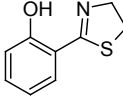
<b>HL1</b>		NBu <sub>4</sub> [Tb( <b>L1</b> ) <sub>4</sub> ]	Tb <b>L1</b> _4
		NBu <sub>4</sub> [Eu( <b>L1</b> ) <sub>4</sub> ]	Eu <b>L1</b> _4
		[Tb( <b>L1</b> ) <sub>3</sub> ] <sub>2</sub>	Tb <b>L1</b> _3
		[Eu( <b>L1</b> ) <sub>3</sub> ] <sub>2</sub>	Eu <b>L1</b> _3
		[Na <sub>2</sub> (Tb( <b>L1</b> ) <sub>3</sub> ) <sub>2</sub> (CO <sub>3</sub> )(dmsO) <sub>2</sub> ] <sub>2</sub>	Tb <b>L1</b> _CO <sub>3</sub>
		[Na <sub>2</sub> (Eu( <b>L1</b> ) <sub>3</sub> ) <sub>2</sub> (CO <sub>3</sub> )(dmsO) <sub>2</sub> ] <sub>2</sub>	Eu <b>L1</b> _CO <sub>3</sub>
<b>HL2</b>		NEt <sub>4</sub> [Tb( <b>L2</b> ) <sub>4</sub> ]	Tb <b>L2</b> _4
		NEt <sub>4</sub> [Eu( <b>L2</b> ) <sub>4</sub> ]	Eu <b>L2</b> _4
		[Tb( <b>L2</b> ) <sub>3</sub> ] <sub>2</sub>	Tb <b>L2</b> _3
		[Eu( <b>L2</b> ) <sub>3</sub> ] <sub>2</sub>	Eu <b>L2</b> _3
		[Eu( <b>L2</b> ) <sub>3</sub> ]	Eu <b>L2</b> _3

Figure 4.1: Schematic overview of the ligands and coordination compounds discussed in this chapter. The rightmost column indicates the designations used.

## 4.2 Experimental

### 4.2.1 General

NMR spectra were recorded on a Bruker DPX-300 spectrometer. Infrared spectra were recorded on a Perkin-Elmer Paragon 1000 FTIR spectrometer equipped with a Golden Gate ATR. Elemental analysis for C, H, N and S was performed on a Perkin-Elmer 2400 series II analyzer. Excitation and emission spectra were recorded on a Shimadzu RF-5301PC spectrofluorophotometer equipped with a solid state sample holder and a UV-blocking filter. Photoluminescence quantum yields were recorded on an Avantes AvaSpec-2048 CCD spectrometer connected to a custom made integrating sphere, based on the AvaSphere 30REFL, using a modification of the absolute method reported by De Mello [19]. A 1000 Watt Xe-discharge lamp and a SPEX monochromator were used as the excitation source. UV-Vis absorption spectra were measured with the same spectrometer, connected to a solid state reflection probe and using an AvaLight DH-S-BAL light source. For determination of luminescence lifetime, an Edinburgh Instruments FLS920 spectrophotometer was used together with a pulsed laser excitation source.

### 4.2.2 X-ray crystallography

Crystals of TbL1\_3, EuL1\_4, EuL1\_CO<sub>3</sub> and TbL1\_CO<sub>3</sub> selected for the X-ray measurements were mounted to the glass fiber using the oil drop method and data were collected at 173 K on a Nonius Kappa CCD diffractometer (Mo-K $\alpha$  radiation, graphite monochromator,  $\lambda = 0.71073 \text{ \AA}$ ) [20]. The intensity data were corrected for Lorentz and polarization effects, and for absorption. The programs COLLECT, SHELXS-97, SHELXL-97 were used for data reduction, structure solution and structure refinement, respectively [21-23]. The non-hydrogen atoms were refined anisotropically. The hydrogen atoms were situated at the calculated positions and refined isotropically riding with the heavy atom connected. EuL1\_CO<sub>3</sub> and TbL1\_CO<sub>3</sub> are isomorphous with one coordinating dmso disordered over two positions with population parameters 0.75 and 0.25. The population parameters of the disordered dmso molecules were fixed during the final least-square cycles. Single crystal structure determination of EuL2\_4 was performed on a STOE IPDS 2T diffractometer, equipped with a Mo-anode (Mo-K $\alpha$  radiation,  $\lambda = 0.71073 \text{ \AA}$ ) as X-ray source, a graphite monochromator and an imaging plate as detector. The data was corrected for Lorentz and polarization effects and for absorption. The programs WinGX and SHELXS-97 were used for crystal structure determination and SHELXL-97 was used for structure refinement [21, 22, 24]. All atomic positions were restrained during refinement and hydrogen atoms were calculated for ideal positions due to the poor crystallinity of the compound.

## 4.2.3 Synthesis

*2-(4,5-dihydro-1,3-oxazol-2-yl)phenol (HL1)*

Following a modification of the procedure reported in [25]. Methyl salicylate (9.13 g, 60 mmol) and 2-aminoethanol (3.62 mL, 60 mmol) were refluxed under argon in a round-bottomed flask for one hour. The methanol that had formed was removed *in vacuo*, leaving the 2-aminoethyl salicylate as highly viscous oil. Subsequently, the oil was dissolved in 150 mL of dichloromethane. The resulting solution was cooled on ice and SOCl<sub>2</sub> (3.8 mL, 63 mmol) was added drop-wise under stirring. The flask was allowed to warm up to room temperature and stirred for 18 hours, resulting in the formation of a white precipitate. The solid compound was separated by filtration and air-dried after which it was taken up in 60 mL of 0.6 M aqueous sodium hydrogen carbonate. The product was extracted with diethyl ether (3 × 90 mL) and obtained as a crystalline solid after drying over magnesium sulfate and evaporation of the solvent. Yield: 5.2 g (32 mmol, 53%). <sup>1</sup>H NMR (300 MHz, dmsO) δ /ppm: 7.64 (dd, *J* = 7.8, 1.8 Hz, 1H), 7.45 (m, 1H), 7.00 (dd, *J* = 8.4, 1.1 Hz, 1H) 6.94 (td, *J* = 7.5, 1.2 Hz, 1H), 4.48 (t, *J* = 9.3 Hz, 2H), 4.07 (t, *J* = 9.3 Hz, 2H). IR (ν/cm<sup>-1</sup>): 2954(w), 2888(w), 1636(m), 1494(m), 1370(m), 1312(m), 1256(m), 1232(m), 1068(m), 938(m), 798(m), 754(s), 678(m), 536(m).

*2-(4,5-dihydro-1,3-thiazol-2-yl)phenol (HL2)*

Following a procedure reported by Minkkilä *et al.* [26]. A neat mixture of 2-hydroxybenzotrionitrile (2.32 g, 19.5 mmol) and 2-aminoethanethiol (2.26 g, 29.3 mmol) was stirred under heating to 100 °C for one hour. After cooling, the mixture was treated with 1.0 M HCl (20 mL) and water (50 mL) and the resulting suspension was extracted with dichloromethane (4 × 70 mL). After drying the organic fraction over magnesium sulfate, the solvent was removed *in vacuo*, leaving the product as yellow needles. Yield, 2.6 g (14 mmol, 73%). <sup>1</sup>H NMR (300 MHz, CDCl<sub>3</sub>) δ /ppm: 7.37 (m, 2H), 6.93 (m, 2H), 4.45 (t, *J* = 8.3 Hz, 2H), 3.34 (t, *J* = 8.3 Hz, 2H). IR (ν/cm<sup>-1</sup>): 2932(w), 2860(w), 1623(w), 1593(s), 1573(m), 1488(s), 1455(m), 1408(m), 1330(m), 1256(m), 1223(s), 1154(m), 1122(m), 1118(m), 1040(m), 1013(s), 956(m), 932(s), 804(s), 754(s), 680(m), 665(m), 613(m), 566(m), 537(w).

*[Tb(L1)<sub>3</sub>]<sub>2</sub> (TbL1\_3)*

HL1 (0.16 g, 1.0 mmol) was dissolved in 20 mL of methanol and 0.50 mL of methanolic NaOH solution (2.0 M) was added. The solution was heated to just below its boiling point, after which a TbCl<sub>3</sub> solution (3.3 mL 0.1 M in methanol) was added. The resulting suspension was refluxed for one hour. The precipitate was filtered and dried *in vacuo* at 60 °C. Yield: 0.19 g (0.29 mmol, 87%) of a white solid. IR (ν/cm<sup>-1</sup>): 2888(w), 1616(m), 1472(s), 1444(m), 1378(m), 1344(m), 1256(m), 1228(m), 1058(m), 856(m), 754(m),

686(m). Elemental analysis calculated (%) for  $C_{27}H_{24}N_3O_6Tb$  ( $[Tb(L1)_3]$ ): C, 50.25; H, 3.75; N, 6.51. Found (%): C, 50.04; H, 3.44; N 6.61.

*[Eu(L1)<sub>3</sub>]<sub>2</sub> (EuL1\_3)*

Following the procedure described for  $TbL1_3$ , but with a 0.1 M methanolic solution of  $EuCl_3$  instead. Yield: 182 mg (0.29 mmol, 86%) of a white solid. IR ( $\nu/cm^{-1}$ ): 2888(w), 1616(m), 1472(s), 1444(m), 1378(m), 1344(m), 1256(m), 1228(m), 1058(m), 856(m), 754(m), 686(m). Elemental analysis calculated (%) for  $C_{27}H_{24}EuN_3O_6$  ( $[Eu(L1)_3]$ ): C, 50.79; H, 3.79; N, 6.58. Found (%): C, 49.46; H, 3.64; N 6.42.

*NBu<sub>4</sub>[Tb(L1)<sub>4</sub>] (TbL1\_4)*

**HL1** (0.16 g, 1.0 mmol) and tetra-n-butylammonium hydroxide (1.2 mL 1 M in methanol) were dissolved in methanol (20 mL) and the solution was heated to just below its boiling point. Next, 2.5 mL of a  $TbCl_3$  solution (0.1 M in methanol) was added and the resulting suspension was refluxed for one hour. The solvent was removed using a rotary evaporator and the remaining solids were rinsed onto a glass filter using demineralized water and dried *in vacuo* at 60 °C. Yield: 0.22 g (0.21 mmol, 83%) of a white solid. IR ( $\nu/cm^{-1}$ ): 2958(w), 2892(w), 1622(s), 1540(w), 1472(s), 1446(m), 1346(s), 1258(m), 1228(m), 754(m). Elemental analysis calculated (%) for  $C_{52}H_{74}N_5O_{11}Tb$  ( $NBu_4[Tb(L1)_4] \cdot 3H_2O$ ): C, 56.57; H, 6.76; N, 6.34. Found (%): C, 55.64; H, 6.62; N 6.25.

*NBu<sub>4</sub>[Eu(L1)<sub>4</sub>] (EuL1\_4)*

Following the procedure described for  $TbL1_4$ , but with a 0.1 M methanolic solution of  $EuCl_3$  instead and starting from 6 mmol (0.98 g) of **HL1**. Yield 1.04 g (1.31 mmol, 88%) of a white powder. IR ( $\nu/cm^{-1}$ ): 2958(w), 1622(s), 1540(m), 1472(s), 1444(s), 1346(s), 1260(m), 1230(m), 1150w, 754(s). Elemental analysis calculated (%) for  $C_{52}H_{68}N_5O_8Tb$  ( $NBu_4[Eu(L1)_4] \cdot 3H_2O$ ): C, 56.93; H, 6.80; N, 6.38. Found (%): C, 56.61; H, 6.88; N 6.29.

*[Tb(L2)<sub>3</sub>] (TbL2\_3)*

Using the procedure for  $TbL1_3$ , starting from 0.60 mmol (107 mg) of **HL2** and 0.20 mmol of  $TbCl_3$ . Yield: 0.10 g (0.074 mmol, 74%) of a white solid. IR ( $\nu/cm^{-1}$ ): 2850(w), 1595(s), 1566(s), 1538(s), 1464(s), 1440(s), 1428(s), 1336(s), 1327(w), 1304(w), 1277(w), 1253(m), 1215(s), 1186(m), 1151(m), 1119(w), 1015(s), 945(m), 853(w), 829(m), 755(s), 744(s), 689(m), 658(m), 624(m), 590(m), 577(m), 530(m), 512(m), 504(m). Elemental analysis calculated (%) for  $C_{27}H_{24}N_3O_3TbS_3$  ( $[Tb(L2)_3]$ ): C, 46.75; H, 3.49; N, 6.06; S, 13.87. Found (%): C, 46.05; H, 3.67; N 6.01; S, 13.40.

*[Eu(L2)<sub>3</sub>] (EuL2\_3)*

Using the procedure reported for  $TbL1_3$ . Yield: 0.10 g (0.074 mmol, 74%) of a yellow powder. IR ( $\nu/cm^{-1}$ ): 2850(w), 1595(s), 1566(s), 1538(s), 1464(s), 1440(s), 1428(s), 1336(s), 1327(w), 1304(w), 1277(w), 1253(m), 1215(s), 1186(m), 1151(m), 1119(w),

1036(w), 1015(s), 945(m), 853(w), 829(m), 755(s), 744(s), 689(m), 658(m), 624(m), 590(m), 577(m). Elemental analysis calculated (%) for  $C_{27}H_{24}EuN_3O_3S_3$  ( $[Eu(L2)_3]$ ): C, 47.23; H, 3.52; N, 6.12; S, 14.01. Found (%): C, 46.34; H, 3.70; N 6.01; S, 13.58.

*NEt<sub>4</sub>[Tb(L2)<sub>4</sub>] (TbL2\_4)*

HL2 (0.106 mg, 0.6 mmol) and tetra-ethylammonium hydroxide (0.42 mL 1.5 M in methanol) were dissolved in methanol (8 mL) and the solution was heated to just below its boiling point. Next, 1.5 mL of a TbCl<sub>3</sub> solution (0.1 M in methanol) was added and the resulting suspension was refluxed for one hour. The solvent was removed using a rotary evaporator and the solids were rinsed onto a glass filter using demineralized water and dried *in vacuo* at 60 °C. Yield: 144 mg (0.14 mmol, 96%) of a white solid. IR ( $v/cm^{-1}$ ): 2850(w), 1595(s), 1575(s), 1532(m), 1464(s), 1442(s), 1428(s), 1392(w), 1343(s), 1325(w), 1257(m), 1210(m), 1178(w), 1148(s), 1122(w), 1036(w), 1005(m), 937(m), 853(w), 829(s), 742(s), 673(m), 652(m), 624(m), 580(m), 530(m), 509(m). Elemental analysis calculated (%) for  $C_{44}H_{52}N_5O_4S_4Tb$  ( $NEt_4[Tb(L2)_4]$ ): C, 52.74; H, 5.23; N, 6.99. Found (%): C, 50.68; H, 5.23; N 6.99.

*NEt<sub>4</sub>[Eu(L2)<sub>4</sub>] (EuL2\_4)*

Following the procedure reported for TbL2\_4. Yield: 149 mg (0.15 mmol, 100%) of a yellow solid. IR ( $v/cm^{-1}$ ): 2850(w), 1595(s), 1575(s), 1532(m), 1464(s), 1442(s), 1428(s), 1392(w), 1343(s), 1325(w), 1257(m), 1210(m), 1178(w), 1148(s), 1122(w), 1036(w), 1005(m), 937(m), 853(w), 829(s), 742(s), 673(m), 652(m), 624(m), 580(m), 530(m), 509(m). Elemental analysis calculated (%) for  $C_{44}H_{52}EuN_5O_4S_4$  ( $NEt_4[Eu(L2)_4]$ ): C, 53.11; H, 5.27; N, 7.04. Found (%): C, 51.43; H, 4.78; N 6.86.

*[Na<sub>2</sub>(Tb(L1)<sub>3</sub>)<sub>2</sub>(CO<sub>3</sub>)(dmsO)<sub>2</sub>]<sub>2</sub> (TbL1\_CO<sub>3</sub>)*

A reaction tube was charged with NaOH (50 mg, 1.25 mmol) and HL1 (163 mg, 1.0 mmol) and 10 mL of dimethylsulfoxide (dmsO) was added. On top of the dmsO layer was added a layer of methanolic solution of TbCl<sub>3</sub> (3.3 mL 0.1 M). The tube was left open to the air and kept undisturbed. Within three weeks, crystals appeared at the interface of the solution. The methanol had evaporated over this period. IR ( $v/cm^{-1}$ ): 3380(w, br), 2973(w), 2902(w), 1622(vs), 1546(m), 1506(m), 1473(vs), 1445(s), 1415(m), 1373(m), 1343(s), 1327(m), 1285(w), 1258(m), 1231(s), 1154(m), 1134(w), 1054(vs), 1036(s), 1013(w), 949(s), 918(w), 850(s), 760(vs), 733(m), 688(s), 659(m), 581(s), 547(w), 535(m). Elemental analysis calculated (%) for  $C_{59}H_{60}N_6Na_2O_{17}S_2Tb_2$  ( $Na_2[Tb(L1)_3]_2(CO_3)(dmsO)_2$ ): C, 45.63; H, 3.89; N, 5.41. Found (%): C, 43.79; H, 3.64; N 5.12.

*[Na<sub>2</sub>(Eu(L1)<sub>3</sub>)<sub>2</sub>(CO<sub>3</sub>)(dmsO)<sub>2</sub>]<sub>2</sub> (EuL1\_CO<sub>3</sub>)*

Following the procedure reported for TbL1\_CO<sub>3</sub>, using a methanolic solution of EuCl<sub>3</sub> (0.1 M) instead of the TbCl<sub>3</sub> solution. IR ( $v/cm^{-1}$ ): 3390(w, br), 2973(w), 2902(w), 1621(vs), 1545(m), 1504(m), 1473(vs), 1444(s), 1409(m), 1372(m), 1341(s), 1284(w), 1257(m),



1230(s), 1214(m), 1153(m), 1128(w), 1053(vs), 1036(s), 948(s), 918(w), 850(s), 760(vs), 730(m), 688(s), 659(m), 580(s), 545(w), 535(m). Elemental analysis calculated (%) for  $C_{59}H_{60}Eu_2N_6Na_2O_{17}S_2$  ( $Na_2(Eu(L1)_3)_2(CO_3)(dmsO)_2$ ): C, 46.04; H, 3.93; N, 5.46. Found (%): C, 44.17; H, 3.45; N 5.25.

## 4.3 Results

### 4.3.1 Synthesis and characterization

The ligands **HL1** and **HL2** were readily obtained in acceptable yields following literature procedures. Several peaks in the IR spectrum of **HL1** are assigned as follows: the signal at  $1643\text{ cm}^{-1}$  (C=N stretch),  $1232\text{ cm}^{-1}$  (C-O stretch phenol) and  $754\text{ cm}^{-1}$  (out of plane C-H bending in 1,2-disubstituted benzene ring). Likewise, the IR spectrum of **HL2** contains signals that are readily assigned to the molecule:  $1593\text{ cm}^{-1}$  (C=N stretch),  $1223\text{ cm}^{-1}$  (C-O stretch phenol) and  $754\text{ cm}^{-1}$  (1,2-disubstituted benzene ring).

The complexes were typically synthesized by refluxing methanolic solutions of the lanthanoid salt, ligand and base mixed in the appropriate ratio. The solutions were heated to ensure complete dissolution of the ligands and to slow down the precipitation of the product. In general, the formation of precipitate was observed when the addition of lanthanoid solution was nearly complete. In general, the synthetic procedures offered the complexes in high yields, ranging between 74% for **EuL2\_3** and **TbL2\_3** to 100% for **EuL2\_4**.

The infrared spectra for the complexes with **L1** show bands due to ligand vibrations. Coordination of the ligand to the metal is evident from the red-shift of several peaks. The free-ligand C=N stretch at  $1643\text{ cm}^{-1}$  for **HL1** is shifted to  $1616\text{ cm}^{-1}$  in the complexes and also the phenol C-O stretch is shifted to a lower frequency in the complexes ( $1228$  vs.  $1232\text{ cm}^{-1}$ ). The IR spectra for **TbL1\_CO3** and **EuL1\_CO3** are similar to of the other complexes with **L1**. The additional strong absorption at  $1050\text{ cm}^{-1}$  can be assigned to the S=O stretching mode of the dmso molecules. For the complexes with **L2**, a shift of the phenol C-O vibration is observed from  $1223\text{ cm}^{-1}$  in the free ligand to  $1215\text{ cm}^{-1}$  in the 1:3 complexes and  $1222\text{ cm}^{-1}$  in the 1:4 complexes. Interestingly, washing of the 1:4 complexes with **L1** and **L2** with demineralized water was found to be the best procedure for removing unreacted materials. Use of cold ethanol gave rise to the formation of complexes with a M:L ratio of 1:3, as found from elemental analysis. Apparently, the tetra-alkyl ammonium salt of the ligand is relatively easily washed out of the 1:4 complexes. Several approaches were undertaken to obtain single crystals of the compounds. Compounds **EuL1\_CO3** and **TbL1\_CO3** were obtained in an attempt to grow single crystals of **EuL1\_3** and **TbL2\_3**. The crystals that have formed indeed show a lanthanoid-to-**L1** ratio of 1:3, but are in fact bimetallic octanuclear compounds containing Na(I) and Ln(III) ions that are tightly bridged by carbonate anions. The only possible source of those carbonate ions is  $CO_2$  captured from the air by the basic solution.

### 4.3.2 Single crystal structure determinations

Experimental data on the crystal structure determination are given in Table 4.1 for compounds TbL1\_3, EuL1\_4, EuL2\_4, EuL1\_CO<sub>3</sub> and TbL1\_CO<sub>3</sub>. Relevant bond lengths and angles for TbL1\_3, EuL1\_4 and EuL2\_4 are given in Table 4.2 and in those for EuL1\_CO<sub>3</sub> and TbL1\_CO<sub>3</sub> are listed in Table 4.3. Note that the quality of the structure determined for EuL2\_4 is low. Hence, it is shown for comparison with EuL1\_4 only. In all compounds, the ligand binds in a bidentate mode to the lanthanoid ion through its phenolate oxygen and the nitrogen atom of the five-membered ring. A projection of the structure of TbL1\_3 is shown in Figure 4.2. It is a dimeric complex in which the Tb(III) ion has a N<sub>3</sub>O<sub>4</sub> coordination sphere. Each Tb ion is surrounded by three chelating ligands; one phenolate oxygen atom of each Tb center forms a bridge between the two metal centers that are related by an inversion center. The coordination geometry around Tb can be described as a distorted pentagonal bipyramid with N1 and O3i on the axial positions. The bond lengths range from 2.445(2) to 2.537(2) Å for Tb-N and from 2.188(1) to 2.369(1) for Tb-O, which is normal for this type of bonds [27]. The distance between the two Tb-centers is 3.7061(6) Å. Projections of the structures of EuL1\_4 and EuL2\_4 are shown in Figure 4.3. The environment around the Eu(III) ion in EuL1\_4 and EuL2\_4 is comprised of four phenolate oxygen atoms and four nitrogen atoms, resulting in an N<sub>4</sub>O<sub>4</sub> coordination sphere. For both compounds, the geometry of the coordination sphere is best described as a distorted trigonal dodecahedron.

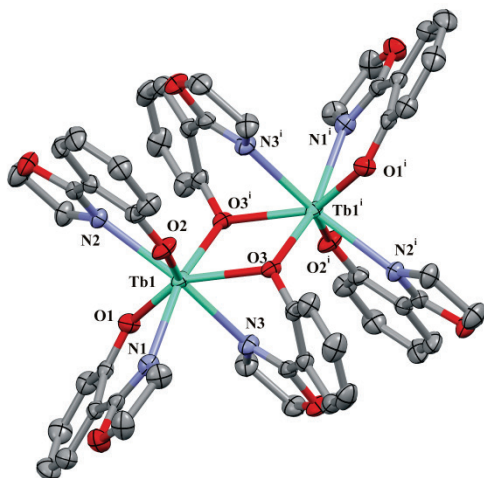


Figure 4.2: Projection of part of the structure of TbL1\_3, shown as 50% probability ellipsoids, with the atom labeling scheme indicated. Hydrogen atoms have been omitted for clarity. The complex is binuclear, with an inversion centre relating the two metal centers. Symmetry operation:  $i: -x, 1 - y, 1 - z$ .

**Table 4.1: Details on the X-ray structure determination of complexes TbL1\_3, EuL1\_4, EuL2\_4, EuL1\_CO<sub>3</sub> and TbL1\_CO<sub>3</sub>.**

	TbL1_3	EuL1_4	EuL2_4	EuL1_CO <sub>3</sub>	TbL1_CO <sub>3</sub>
formula	C <sub>54</sub> H <sub>48</sub> EuN <sub>6</sub> O <sub>12</sub>	C <sub>52</sub> H <sub>68</sub> EuN <sub>5</sub> O <sub>8</sub>	C <sub>44</sub> H <sub>52</sub> EuN <sub>5</sub> O <sub>4</sub> S <sub>4</sub>	C <sub>59</sub> H <sub>60</sub> Eu <sub>2</sub> N <sub>6</sub> Na <sub>2</sub> O <sub>17</sub> S <sub>2</sub>	C <sub>59</sub> H <sub>60</sub> N <sub>6</sub> Na <sub>2</sub> O <sub>17</sub> S <sub>2</sub> Tb <sub>2</sub>
fw	1290.82	1043.07	995.11	1539.17	1553.11
crystal size [mm <sup>3</sup> ]	0.20×0.20×0.15	0.20×0.20×0.17	n.d.	0.15×0.15×0.10	0.25×0.25×0.20
crystal color	Colorless	Colorless	Colorless	Colorless	Colorless
crystal system	Triclinic	Monoclinic	Monoclinic	Monoclinic	Monoclinic
space group	P-1 (# 2)	P2 <sub>1</sub> /c (# 14)	P2 <sub>1</sub> /c (# 14)	P2 <sub>1</sub> /n (# 14)	P2 <sub>1</sub> /n (# 14)
a [Å]	10.142(1)	13.818(2)	10.888(3)	13.631(5)	13.613(2)
b [Å]	15.445(1)	19.342(5)	24.875(8)	25.174(6)	25.110(5)
c [Å]	11.644(2)	19.720(3)	17.698(4)	18.252(5)	18.264(2)
α [°]	85.44(1)	90	90	90	90
β [°]	89.43(1)	108.04(3)	106.85(2)	99.31(3)	99.69(1)
γ [°]	82.26(1)	90	90	90	90
V [Å <sup>3</sup> ]	1218.4(3)	5011.4(19)	4588(2)	6181(3)	6154.0(2)
Z	1	4	4	4	4
d <sub>calc</sub> [g/cm <sup>3</sup> ]	1.759	1.383	1.441	1.654	1.676
μ [mm <sup>-1</sup> ]	2.951	1.309	1.595	2.167	2.436
refl.					
measured / unique parameters	20239/5560	64982/8814	16846/7864	97939/14138	68166/10746
R1/wR2	0.0165/0.0415	0.0378/0.0829	0.1608/ 0.3868	0.0457/0.0707	0.0370/0.0687
[I>2σ(I)]					
R1/wR2 [all refl.]	0.0191/0.0428	0.0597/0.0977	0.2259/0.424	0.0753/0.0779	0.0473/0.0717
S	1.08	1.11	1.27	1.10	1.21
P <sub>min</sub> /max [e/Å <sup>3</sup> ]	-0.53/0.62	-0.55/2.75	4.00/-3.30	-0.59/1.54	-0.62/1.52

For EuL1\_4, the bond lengths range from 2.575(4) to 2.620(3) Å for Eu-N and from 2.311(3) to 2.337(3) Å for Eu-O. For The Eu-N bond lengths in EuL2\_4 range from 2.50(3) to 2.68(3) Å while the Eu-O bonds vary between 2.24(3) and 2.28(1) Å. The latter bond lengths are substantially shorter than the Eu-O bonds in EuL1\_4, which might be due to the strong compression of the [Eu(L2)<sub>4</sub>]<sup>-</sup> complex ion along the crystallographic a-axis. Otherwise, comparable values are known in literature [27]. In both compounds, the alkyl groups of the tetraalkyl-ammonium cation occupy the interspace between two ligands coordinated to the Eu(III) ion.

Compounds TbL1\_CO<sub>3</sub> and EuL1\_CO<sub>3</sub> are isostructural, and are both described as bimetallic octanuclear complexes. The structures contain two independent sodium ions and two independent lanthanoid ions; the other four metal ions are related by an inversion center. A projection of the symmetry-independent part of TbL1\_CO<sub>3</sub> is shown in

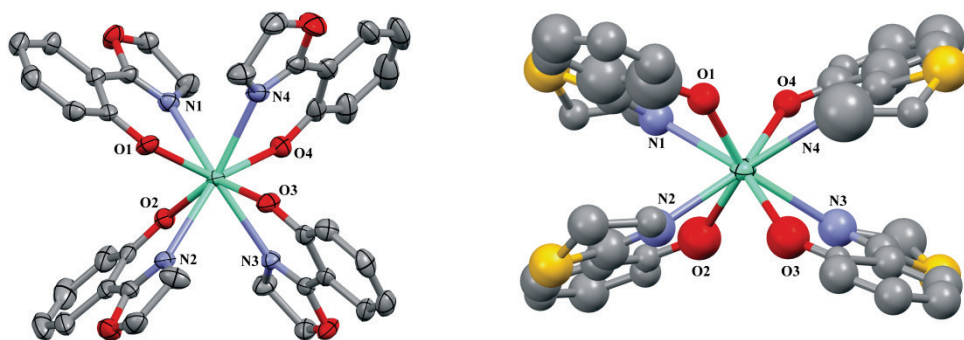


Figure 4.3: Projections of the structures of **EuL1\_4** (left) and **EuL2\_4** (right), with the atom labeling schemes indicated. Hydrogen atoms have been omitted for clarity. The structure of **EuL1\_4** is shown as 50% probability ellipsoids; the structure of **EuL2\_4** is shown as 30% probability ellipsoids. In both compounds, the geometry around the central ion is best described as a distorted trigonal dodecahedron.

Figure 4.4. A wireframe diagram showing the connectivity of the metal centers is given in Figure 4.5. In **TbL1\_CO<sub>3</sub>** and **EuL1\_CO<sub>3</sub>**, each *Ln* ion is surrounded by three ligands **L1** binding in a bidentate mode. The two independent *Ln* centers (*Ln1* and *Ln2*) are bridged by O91 of the carbonate ion. The resulting bond is almost linear (*Ln1*-O91-*Ln2* = 172.7(1)° and 172.1(1)° for **TbL1\_CO<sub>3</sub>** and **EuL1\_CO<sub>3</sub>**). The Na1 ion connects through a third bond of O91. The carbonate ion chelates each *Ln* ion; the resulting *Ln1*-CO<sub>3</sub>-*Ln2* moiety is quasi-planar. The remaining edge of the carbonate ion chelates the Na2 ion through O92 and O93. Two phenol oxygen atoms of each *Ln* center bridge to the Na1 ion, while only one phenol oxygen (O312) bridges the *Ln1* and Na2 ions. The O93 atom forms a bridge between Na2 and the symmetry related Na2<sup>i</sup> ion at a nearly right angle (Na2-O93-Na2<sup>i</sup> = 88.8(1)° and 89.9(1)° for **TbL1\_CO<sub>3</sub>** and **EuL1\_CO<sub>3</sub>**). Thus, Na2-O93-Na2<sup>i</sup>-O93<sup>i</sup> defines a slightly distorted rectangle with an inversion center at its midpoint generating the other half of the molecule. Both lanthanoid sites have an N<sub>3</sub>O<sub>5</sub> coordination sphere that can be described as a distorted trigonal dodecahedron. *Ln*-N distances range from 2.522(4) to 2.560(4) Å for **EuL1\_CO<sub>3</sub>** and from 2.483(4) to 2.538(4) Å for **TbL1\_CO<sub>3</sub>**; *Ln*-O bond distances vary from 2.257(3) to 2.544(3) Å and from 2.237(3) to 2.483(3) Å for **EuL1\_CO<sub>3</sub>** and **TbL1\_CO<sub>3</sub>**, respectively. In both compounds, the bonds between the lanthanoid ion and the carbonate oxygen atoms are substantially longer than the bonds to the phenolate oxygens. In addition, the Na1 ion resides in a six coordinated site, with the geometry resembling a distorted octahedron. The Na2 ion resides in a five-fold coordination site, which is best described as a distorted trigonal bipyramid. Na-O bond lengths in **EuL1\_CO<sub>3</sub>** range from 2.279(4) to 2.759(4) Å and from 2.287(4) to 2.792(4) Å in **TbL1\_CO<sub>3</sub>**. In both **EuL1\_CO<sub>3</sub>** and **TbL1\_CO<sub>3</sub>**, disorder is found for the dmsO attached to Na2. In both cases, the molecule is disordered over two positions, with relative occupancies of 0.75 and 0.25.

**Table 4.2: Selected bond distances (Å) and angles (°) for TbL1\_3, EuL1\_4 and EuL2\_4. Atom labeling is shown in Figure 4.2 for TbL1\_3 and in Figure 4.3 for EuL1\_4 and EuL2\_4.**

	TbL1_3	EuL1_4	EuL2_4
<i>Bond distance (Å)</i>			
<i>Ln-N1</i>	2.445(2)	2.597(4)	2.50(3)
<i>Ln -N2</i>	2.468(2)	2.620(3)	2.59(2)
<i>Ln -N3</i>	2.537(2)	2.575(4)	2.69(3)
<i>Ln -N4</i>		2.611(4)	2.67(3)
<i>Ln -O1</i>	2.188(1)	2.311(3)	2.26(2)
<i>Ln -O2</i>	2.194(1)	2.337(3)	2.24(3)
<i>Ln -O3</i>	2.369(1)	2.331(3)	2.26(3)
<i>Ln -O3<sup>i</sup></i>	2.300(1)		
<i>Ln -O4</i>		2.316(3)	2.28(1)
C15-C16	1.453(3)	1.479(6)	1.46(4)
C25-C26	1.444(3)	1.467(8)	1.48(4)
C35-C36	1.453(3)	1.473(6)	1.48(5)
C45-C46		1.458(8)	1.47(3)
<i>Bond angle (°)</i>			
N1- <i>Ln</i> -O1	73.54(5)	70.6(1)	65(1)
N2- <i>Ln</i> -O2	72.27(5)	69.5(1)	64.5(8)
N3- <i>Ln</i> -O3	67.32(5)	70.2(1)	68.5(8)
O4- <i>Ln</i> -N4		69.9(1)	63(1)
Tb-O3-Tb <sup>i</sup>	105.08(5)		
O3-Tb-O3 <sup>i</sup>	74.92(5)		

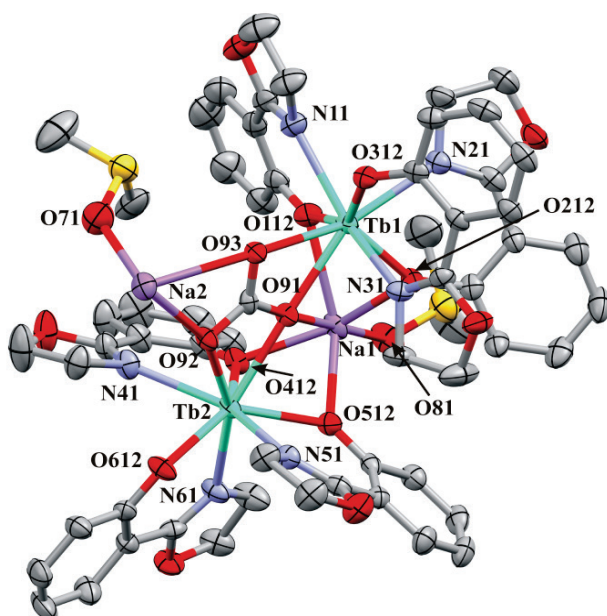


Figure 4.4: Projection of half a molecule of TbL1\_CO<sub>3</sub> shown as 50% probability ellipsoids, with the atom labeling scheme indicated. Hydrogen atoms have been removed for clarity, and only the major component of the disordered dmso molecule is shown.

**Table 4.3: Selected bond distances (Å) and angles (°) for EuL1\_CO<sub>3</sub> and TbL1\_CO<sub>3</sub>. Atom labeling is shown in Figure 4.4.**

EuL1_CO <sub>3</sub>		TbL1_CO <sub>3</sub>	EuL1_CO <sub>3</sub>		TbL1_CO <sub>3</sub>	
<i>Bond distance</i> (Å)			<i>Bond angle</i> (°)			
<i>Ln1-N1</i>	2.560(4)	2.538(4)	<i>O1-Ln1-N1</i>	70.6(1)	71.3(1)	
<i>Ln1-N2</i>	2.522(4)	2.500(4)	<i>O2-Ln1-N2</i>	71.4(1)	71.8(1)	
<i>Ln1-N3</i>	2.546(4)	2.513(4)	<i>O3-Ln1-N3</i>	68.0(1)	68.6(1)	
<i>Ln1-O1</i>	2.296(3)	2.277(3)	<i>O4-Ln2-N4</i>	69.5(1)	70.3(1)	
<i>Ln1-O2</i>	2.301(3)	2.285(3)	<i>O5-Ln2-N5</i>	69.6(1)	70.3(1)	
<i>Ln1-O3</i>	2.344(3)	2.318(3)	<i>O6-Ln2-N6</i>	71.9(1)	72.7(1)	
<i>Ln1-O91</i>	2.493(3)	2.483(3)				
<i>Ln1-O93</i>	2.498(3)	2.470(3)	<i>Ln1-O3-Na2<sup>i</sup></i>	97.6(1)	98.2(1)	
<i>Ln2-N4</i>	2.536(4)	2.514(4)	<i>Ln1-O93-Na2<sup>i</sup></i>	97.8(1)	98.5(1)	
<i>Ln2-N5</i>	2.543(4)	2.513(4)	<i>O93-Ln1-O3</i>	78.95(9)	79.0(1)	
<i>Ln2-N6</i>	2.514(4)	2.483(4)	<i>O93-Na2<sup>i</sup>-O3</i>	81.3(1)	80.3(1)	
<i>Ln2-O4</i>	2.311(3)	2.281(3)	<i>Na2-O93-Na2<sup>i</sup></i>	89.9(1)	88.8(1)	
<i>Ln2-O5</i>	2.329(3)	2.308(3)	<i>O93-Na2-O93<sup>i</sup></i>	90.1(1)	91.2(1)	
<i>Ln2-O6</i>	2.257(3)	2.237(3)				
<i>Ln2-O91</i>	2.544(3)	2.516(3)	<i>Ln1-O91-C91</i>	94.4(2)	93.6(2)	
<i>Ln2-O92</i>	2.484(3)	2.465(3)	<i>Ln2-O91-C91</i>	92.8(2)	92.8(2)	
<i>Na1-O81</i>	2.473(3)	2.287(4)	<i>Ln1-O91-Ln2</i>	172.1(1)	172.7(1)	
<i>Na1-O91</i>	2.279(4)	2.464(3)	<i>Na1-O91-Ln1</i>	88.0(1)	88.0(1)	
<i>Na1-O1</i>	2.657(3)	2.630(4)	<i>Na1-O91-Ln2</i>	84.12(9)	84.8(1)	
<i>Na1-O2</i>	2.356(3)	2.345(3)				
<i>Na1-O4</i>	2.346(3)	2.337(4)				
<i>Na1-O5</i>	2.422(3)	2.412(3)				
<i>Na2-O92</i>	2.316(3)	2.325(4)				
<i>Na2-O93</i>	2.759(4)	2.792(4)				
<i>Na2-O71</i>	2.37(4)	2.37(4)				

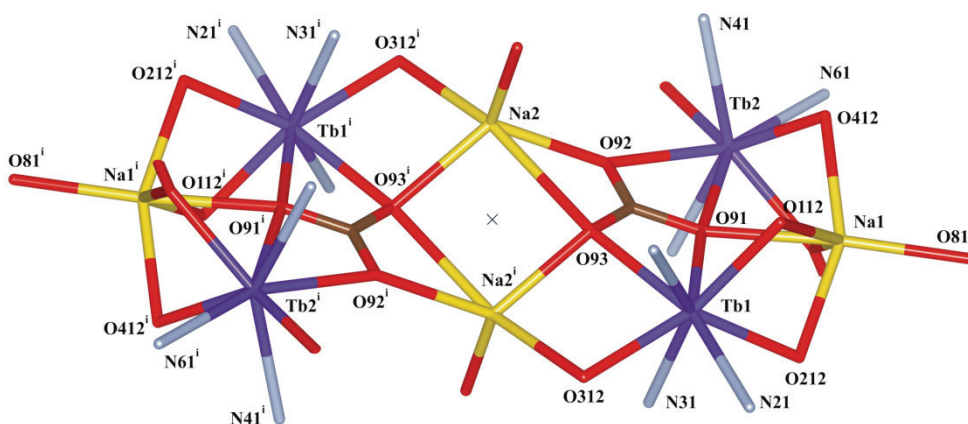


Figure 4.5: Wireframe representation of the structure of TbL1\_CO<sub>3</sub> showing the connectivity of the metal centers. The position of the inversion center is indicated by a cross. Symmetry operation: *i*) 1 - *x*, -*y*, -*z*.

### 4.3.3 Luminescence

All compounds show photoluminescence upon excitation in the near-UV region. Photoluminescence emission and excitation spectra are shown in Figure 4.6. Excitation spectra were obtained by constantly monitoring the intensity of the strongest emission line, i.e. the  $^5D_0 \rightarrow ^7F_2$  transition for Eu(III) compounds and the  $^5D_4 \rightarrow ^7F_5$  transition for Tb(III) compounds, while scanning the excitation wavelength from 220 to 420 nm. The Eu(III) complexes all exhibit luminescence characteristic for the Eu(III) ion, with transitions from the  $^5D_0$  resonance level to the  $^7F_J$  manifold around 590, 614, 650 and 700 nm for  $J = 1, 2, 3$  and 4, respectively [28]. In all cases, the most dominant line is the  $^5D_0 \rightarrow ^7F_2$  transition. Only weak luminescence is observed for EuL1\_CO<sub>3</sub>; luminescence intensities of EuL1\_3, EuL2\_3 are even lower and their spectra are not included. The excitation spectra show broad bands extending into the near-UV region. All three Eu compounds have an excitation band at 290 nm and a second distinct band at 370 nm. In the excitation spectrum of EuL2\_3, a band appears around 340 nm, while EuL1\_CO<sub>3</sub> has an additional band centered at 396 nm.

The emission spectra recorded for the Tb(III) compounds all show lines characteristic for transitions from the  $^5D_4$  level of Tb(III) to the  $^7F_J$  manifold, at 488, 545, 585 and 627 nm for  $J = 6, 5, 4$  and 3 [29]. In all cases, the strongest line corresponds to the  $^5D_4 \rightarrow ^7F_5$  transition. The excitation spectra for the Tb(III) complexes with L1 appear to be composed of three distinct bands of roughly equal intensity centered at 295, 325 and 370 nm. The excitation spectrum of TbL1\_CO<sub>3</sub> is similar to the one recorded for TbL1\_3 and has nearly constant intensity between 295 and 375 nm, whereas the 370 nm band for TbL1\_4 is slightly more intense. The photoluminescence quantum yields and experimental luminescence lifetimes of the complexes are given in Table 4.4.

**Table 4.4: Photophysical properties of the Eu(III) and Tb(III) complexes.**

Compound	$\Phi_{\text{tot}}$ (%)	$\Omega_2$ ( $10^{-20}$ cm <sup>2</sup> )	$\Omega_4$ ( $10^{-20}$ cm <sup>2</sup> )	$\tau_{\text{exp}}$ (ms)	$\tau_{\text{rad}}$ (ms)	$\Phi_{Ln}$ (%)	$\eta_{\text{sens}}$ (%)
EuL1_3	n.d.	n.d.	n.d.	n.d.	n.d.	n.d.	n.d.
TbL1_3	38	n.d.	n.d.	0.47	n.d.	n.d.	n.d.
EuL1_4	43	20.7	2.57	0.67	1.40	48	90
TbL1_4	79	n.d.	n.d.	0.66	n.d.	n.d.	n.d.
EuL2_3	n.d.	n.d.	n.d.	n.d.	n.d.	n.d.	n.d.
TbL2_3	16	n.d.	n.d.	0.03	n.d.	n.d.	n.d.
EuL2_4	20	17.5	5.1	0.33	1.51	22	91
TbL2_4	3	n.d.	n.d.	n.d.	n.d.	n.d.	n.d.
EuL1_CO <sub>3</sub>	n.d.	n.d.	n.d.	n.d.	n.d.	n.d.	n.d.
TbL1_CO <sub>3</sub>	51	n.d.	n.d.	n.d.	n.d.	n.d.	n.d.

$\Phi_{\text{tot}}$ : Overall photoluminescence quantum yield at 360 nm excitation,  $\tau_{\text{exp}}$ : experimental lifetime of the emissive state of the Ln(III) ion,  $\Omega_J$  intensity parameters,  $\tau_{\text{rad}}$ : radiative lifetime of the  $^3D_0$  state of Eu(III),  $\Phi_{Ln}$ : intrinsic quantum yield,  $\eta_{\text{sens}}$ : sensitizer efficiency.

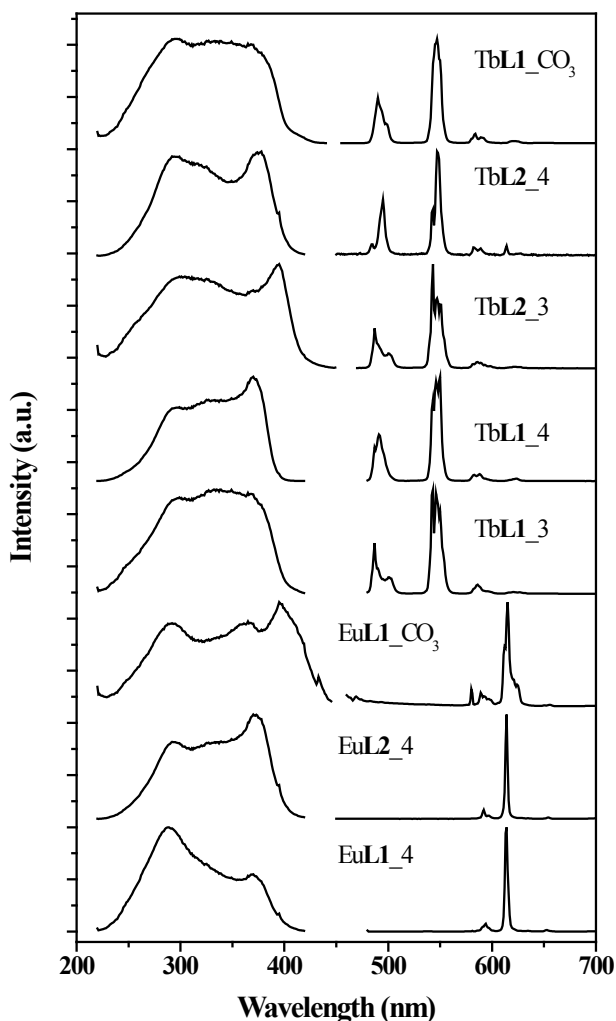


Figure 4.6: Photoluminescence spectra of the Eu(III) compounds **EuL1\_4**, **EuL2\_4** and **EuL1\_CO3** (bottom) and of the Tb(III) compounds **TbL1\_3**, **TbL1\_4**, **TbL2\_3**, **TbL2\_4** and **TbL1\_CO3** (top). The excitation spectra ( $\lambda_{em} = 614$  nm for Eu(III) compounds and  $\lambda_{em} = 545$  nm for Tb(III) compounds) are shown on the left hand side while the right hand side shows the emission spectra ( $\lambda_{exc} = 360$  nm) of the compounds. The emission lines at 595, 614, 649 and 685 nm correspond to the  ${}^5D_0 \rightarrow {}^7F_J$ ,  $J = 1, 2, 3, 4$  transitions of the Eu(III) ion. The emission lines at 495, 545, 580 and 625 nm are characteristic of the Tb(III) ion, corresponding to the  ${}^3D_4 \rightarrow {}^7F_J$ ,  $J = 6, 5, 4, 3$  transitions.

For the Eu-complexes, the luminescence intensity of **EuL1\_3**, **EuL2\_3** and **EuL1\_CO3** was too weak to allow for reliable determination of quantum yields. For **EuL1\_4**, a quantum yield of 43% and a lifetime of 0.67 ms were recorded. For the Tb(III) complexes, solid state photoluminescence quantum yields range from 3% for **TbL2\_3** to 79% for **TbL1\_4**. The luminescence lifetimes for these complexes are 0.33 and 0.66 ms, respectively.



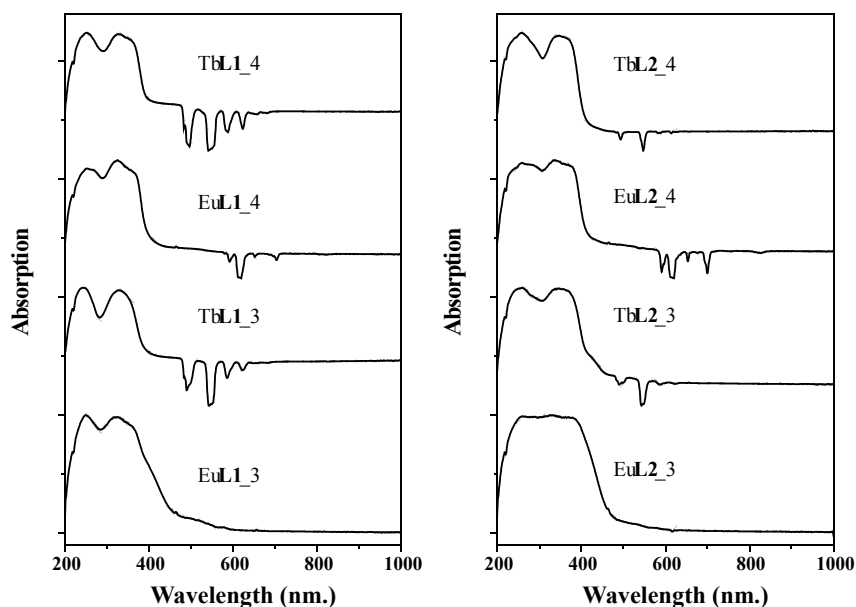


Figure 4.7: Absorption spectra recorded for LnL1<sub>x</sub> compounds (left) and LnL2<sub>x</sub> compounds (right). The downward pointing peaks result from luminescence of the compounds upon excitation in the nUV.

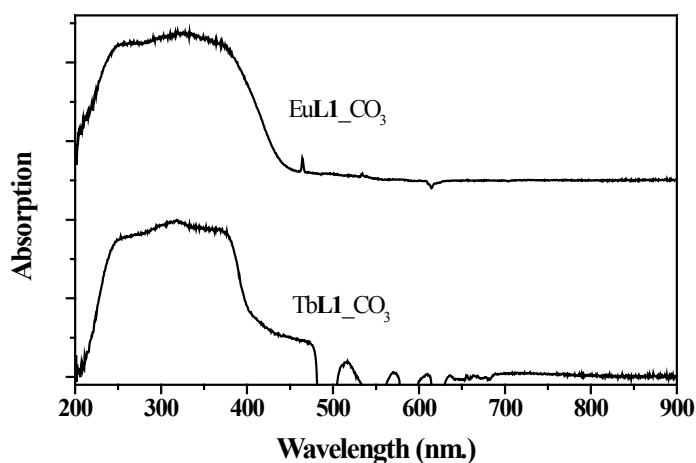


Figure 4.8: Absorption spectra recorded for LnL1<sub>CO<sub>3</sub></sub> compounds. The downward pointing peaks result from luminescence of the compounds upon excitation in the nUV.

#### 4.3.4 Absorption spectra

The absorption spectra of the compounds are given in Figure 4.7 and Figure 4.8. The absorption spectra all feature broad absorption bands in the nUV region, and two bands

may be distinguished; one centered at 250 nm and one around 330 nm. The shapes of absorption bands are roughly the same as observed in the excitation spectra, indicating ligand sensitization of the lanthanoid emission in these complexes.

## 4.4 Discussion

### 4.4.1 Single crystal structure determinations

In the compounds with a *Ln*(III) to ligand ratio of 1:4, the ligand is able to saturate the coordination sphere around the lanthanoid ion. In the TbL1\_3 complex with a 1:3 *Ln*(III)-to-ligand ratio, the coordination sphere of the Tb(III) ion is saturated by forming a di- $\mu$ -phenolato bridge between two adjacent Tb(III) ions, which results in an increased coordination number. The formation of bridges between two lanthanoid ions is not uncommon, and has been reported for phenolates, chlorides, acetates and benzoates [30-35]. Interestingly, there is a significant difference between the Tb-O bond lengths of the bridging phenolate. Both bonds are somewhat longer than the Tb-O bonds to the non-bridging phenolates, but the bridging Tb-O3<sup>i</sup> bond (2.300(1) Å) is actually shorter than the chelating Tb-O3 bond (2.369(1) Å). The asymmetry of the  $\mu$ -phenolato bridge is larger than reported in previous studies [30, 34].

The structures of compounds EuL1\_4 and EuL2\_4 are highly similar, although the structure of the latter complex is compressed along the crystallographic *a*-axis. The packing is similar in both cases, involving packing along the crystallographic *y*-axis of alternating [EuL<sub>4</sub>]<sup>-</sup> ions and NR<sub>4</sub><sup>+</sup> ions. In EuL2\_4, CH- $\pi$  stacking appears to be present between the terminal methyl groups of the cation and the benzene rings of the ligands with an average carbon- $\pi$ -plane distance of approximately 3.6 Å [36]. Such interactions appear to be present as well in between the NBu<sub>4</sub><sup>+</sup> cations and the [EuL<sub>4</sub>]<sup>-</sup> complexes in EuL1\_4.

In EuL1\_CO<sub>3</sub> and TbL1\_CO<sub>3</sub>, the phenol-oxygens O112-O512 form a bridge between the *Ln*(III) and Na centers. In all cases, the Ln-O bond is shorter than the Na-O bond, due to the slightly larger ionic radius of the sodium ion. As can be seen from Figure 4.5, the slightly distorted rectangle defined by Na2, O93 and the equivalent Na2<sup>i</sup> and O93<sup>i</sup> atoms is at the center of the structure. Attached on two opposing sides of this rectangle is a distorted rhombus defined by Tb1, O3, Na2<sup>i</sup> and O93, with O-M-O, (M = Na, *Ln*) angles < 90° and obtuse *Ln*-O-Na angles. The carbonate ions form an important center in the structure, connecting all metal centers in the asymmetric unit of the molecule as well as connecting the asymmetric units leading to the formation of an octanuclear complex. The capture of CO<sub>2</sub> from the air resulting in the formation of a bridging carbonate ion has been reported before for the synthesis of *Ln*(III) compounds [37-40]. Also in other reports, where the carbonate ion is purposely added [41, 42] or formed upon decomposition of one of the reagents [43-45], the CO<sub>3</sub><sup>2-</sup> ion acts as an important linker in the structure.

#### 4.4.2 Luminescence

##### *Photoluminescence spectra*

The broad excitation bands recorded for all luminescent compounds clearly indicate that both **L1** and **L2** are acting as antennae that sensitize the lanthanoid-centered emission. The emission spectra of the Eu(III) compounds are all dominated by the  $^5D_0 \rightarrow ^7F_2$  transition around 614 nm. The fact that the intensity of the  $^5D_0 \rightarrow ^7F_2$  transition, which is of forced electric dipole (ED) nature, is much higher than that of the  $^5D_0 \rightarrow ^7F_1$  magnetic dipole (MD) transition indicates that the Eu(III) ion is situated in a non-centrosymmetric environment [46-48]. This is in agreement with the structures determined for Eu**L1**\_4, Eu**L2**\_4 and Eu**L1**\_CO<sub>3</sub>. For the Eu(III) complexes, the excitation spectra appear to vary markedly between the compounds. For Eu**L1**\_4, the band around 370 nm is the weakest, while it is the strongest band in the excitation spectrum of Eu**L2**\_4. For Eu**L1**\_CO<sub>3</sub>, an additional strong band centered at 395 nm appears. Because ligand-centered excitation in this compound is only very weak, direct excitation of the Eu(III) ion is comparatively strong. Consequently, this band may arise from the overlap of the  $(^5L_6, ^5G_2, ^5L_7, ^5G_3) \leftarrow ^7F_0$  transitions of Eu(III) around 395 nm, with a weak ligand-centered band. The emission spectra of Tb**L1**\_3, Tb**L1**\_4, Tb**L2**\_3, Tb**L2**\_4 and Tb**L1**\_CO<sub>3</sub> are similar and are dominated by the Tb(III)  $^5D_4 \rightarrow ^7F_5$  transition around 546 nm. The different splitting patterns of the emission lines are a result of crystal field splitting of the free ion  $^7F_J$  level. Comparing the excitation spectra for the Tb(III) complexes sensitized by the **L1** ligand shows that those for Tb**L1**\_3 and Tb**L1**\_CO<sub>3</sub> are highly similar, while for Tb**L1**\_4 the intensity of the band at 374 nm is slightly enhanced. The enhanced long-wavelength band is also seen for Tb**L2**\_3 and Tb**L2**\_4, for which the excitation spectra are nearly identical. Similar appearances of excitation spectra for a given ligand are as expected, because they depend on the ligand-centered energy levels. These, in turn, can vary slightly between complexes as a result of slight differences in structure.

##### *Luminescence efficiency*

In this study, the metal-to-ligand ratio is found to have a strong impact on the luminescence efficiency of the complexes. For example Eu**L1**\_3 and Eu**L1**\_CO<sub>3</sub> are practically non-luminescent while Eu**L1**\_4 shows relatively bright luminescence with a quantum yield of 43%. Similarly, Eu**L2**\_3 is not luminescent while Eu**L2**\_4 shows moderately bright luminescence with a quantum efficiency of 20%. Thus, only the Eu(III) complexes with a 1:4 lanthanoid-to-ligand ratio show visible luminescence. The Tb**L1**\_3, Tb**L1**\_4 and Tb**L1**\_CO<sub>3</sub> complexes all show moderate to strong photoluminescence, with the quantum efficiency for Tb**L1**\_4 compound being as high as 79%. The improved efficiency of Tb**L1**\_4 as compared to Tb**L1**\_3 is also reflected in the increased lifetime, indicating that the contribution of non-radiative processes has decreased. For Tb(III) compounds with the ligand **L2**, the behavior with respect to changes in the M:L ratio is reversed compared to

those with **L1**. Thus, Tb**L2**\_3 shows moderately intense luminescence with a quantum yield of 16%, while Tb**L2**\_4 shows only very weak luminescence. Overall, the ligand **L2** is not as good an antenna for Tb(III) as is the **L1** ligand.

In general, the luminescence lifetime is shorter for complexes with lower overall luminescence quantum yields. This is readily explained by the larger relative contribution of non-radiative pathways depopulating the  $Ln(III)$  excited state, resulting in lowering of the intrinsic quantum yield of the ion [49, 50]. For compounds based on the Eu(III) ion, the intrinsic quantum yield is readily calculated if the experimental lifetime is known and an emission spectrum representing the relative photon flow is available [51, 52]. With  $A_{rad}$  and  $A_{nr}$  representing the radiative and non-radiative depopulation rate constants, respectively, the intrinsic quantum yield  $\Phi_{Ln}$  is given by equation 1.

$$\Phi_{Ln} = \frac{A_{rad}}{A_{rad} + A_{nr}} \quad (1)$$

The intrinsic quantum yields for the Eu(III) ion in Eu**L1**\_4 and Eu**L2**\_4 are given in Table 4.4. It appears that the main difference in overall quantum yield is largely the result of different intrinsic quantum yields of the Eu(III) ion among the two compounds; the quantum efficiency for Eu**L2**\_4 is half that of Eu**L1**\_4, and so is its luminescence lifetime: 0.33 ms vs. 0.67 ms. An expression for the overall photoluminescence quantum yield  $\Phi_{tot}$  may be written as equation 2.

$$\Phi_{tot} = \eta_{sens} \times \Phi_{Ln} \quad (2)$$

With  $\Phi_{Ln}$  representing the intrinsic quantum yield given in equation 1 and  $\eta_{sens}$  representing the sensitizer efficiency, which contains contributions of the ligand-centered intersystem crossing efficiency and ligand-to-metal energy transfer energy, this equation can be used to assess the antenna efficiency of the ligands. From Table 4.4 it can be seen that for Eu**L1**\_4 and Eu**L2**\_4, the sensitizer efficiency is practically the same for both ligands. Because the 1:4 M:L Eu(III) complexes both show intense luminescence, the lack of efficient metal-centered photoluminescence for Eu**L1**\_3, Eu**L2**\_3 and Eu**L1**\_CO<sub>3</sub> cannot be attributed to the ligand-centered triplet excited state being too low in energy. In addition, no residual ligand-centered phosphorescence is observed. It is known that in Eu(III) complexes a low-lying ligand-to-metal charge transfer band can be present. The charge transfer band in turn can compete with the ligand-to-metal energy transfer, thereby effectively quenching lanthanoid-centered luminescence [53-56]. The presence of such state can be identified from absorption spectra, which are shown in Figure 4.7 for the  $LnL1_x$  and  $LnL2_x$ , ( $x = 1, 2$ ) complexes and in Figure 4.8 for the  $LnL1\_CO_3$  compounds [57]. Superficially, all absorption spectra look highly similar, with equal-intensity bands around 250 nm and 350 nm. Indeed, compared to the Tb(III) complexes, the long wavelength absorption band for the 1:3 Eu(III) complexes extends slightly further into the blue spectral region. This

additional band around 400 nm indicates the presence of a charge transfer band for EuL1\_3 and EuL2\_3. Also, comparing the absorption spectra of EuL1\_CO<sub>3</sub> and TbL1\_CO<sub>3</sub> reveals that the absorption spectrum of EuL1\_CO<sub>3</sub> extends further into the visible region. It seems that the structure of the 1:3-compounds is better capable of stabilizing the divalent state of the Eu-ion than the 1:4 structure. Lowering of the LMCT state in an Eu(III) complex as a result of a different M:L ratio has been reported before and appears to be responsible for quenching the Eu(III)-centered emission in the 1:3 complexes [53]. It appears that generally, phenol-type ligands fail to excite luminescence of the Eu(III) ion. For example, 4-hydroxyisophthalate is able to sensitize emission of the Tb(III) ion, while the analogous Eu(III) complex is non luminescent [58]. Similarly, complexes of Eu(III) with salicylate-type ligands were found to be weakly or even non-luminescent, while their Tb(III) analogues show bright luminescence [18]. This is readily understood from the ability of phenolates to form phenoxyl radicals upon oxidation [59]. Because the Eu ion has a stable divalent state, a low lying charge transfer band may occur in such compounds, quenching the luminescence [54]. Indeed, it is found that 3,5-dinitrosalicylate is an efficient sensitizer for Eu(III) luminescence [13, 60]. In this ligand, the two strongly electron-withdrawing groups raise the level of the LMCT state sufficiently to prevent competition between the LMCT state and L\* → Eu(III) energy transfer. Although L1 and L2 described in this chapter do not bear such strongly electron-withdrawing groups, luminescence of the complexes with the 1:4 Eu:L ratio is not hindered by a low energy LMCT state. This mechanism of quenching is usually not present in Tb(III) complexes as the Tb ion has no stable divalent state, and as a result, all Tb(III) complexes show photoluminescence. The weak emission intensity of the TbL2 complexes compared to the TbL1 complexes might be due to a poor spectral match between the ligand L2 and the Tb(III) ion.

## 4.5 Conclusion

Ten new complexes of Eu(III) and Tb(III) ions, using phenol oxazoline or phenol thiazoline in M:L ratios of 1:3 and 1:4 have been synthesized in yields ranging from 74% to 100%. The complexes show luminescence characteristic of the lanthanoid ion upon excitation in the nUV spectral region, the intensity of which is strongly influenced by the M:L ratio. Solid state photoluminescence studies on the complexes indicate that L1 can sensitize luminescence of the Tb(III) ion in both 1:3 and 1:4 M:L ratios, with the 1:4 ratio giving the most intense photoluminescence. The same ligand only sensitizes Eu(III) centered luminescence in a M:L ratio of 1:4. The presence of an LMCT state in the 1:3 complexes appears to be responsible for quenching the luminescence. The ligand L2 is a less effective antenna for sensitizing Eu(III) and Tb(III) luminescence; the 1:4 M:L Eu(III) complex shows moderately intense luminescence, whereas the 1:3 complex does not. The 1:3 M:L ratio appears to stabilize an LMCT state in the Eu(III) complexes, which in turn quenches Eu-centered luminescence. This shows that not only the ligand centered energy levels determine the photoluminescence efficiency of the complex, but also the M:L ratio should

be taken into consideration. The long-wavelength excitation maximum of EuL1\_4 combined with a moderately high quantum yield show that this class of ligands is promising as sensitizer for Eu(III) and Tb(III) ions. Due to its long-wavelength excitation maximum and high photoluminescence quantum efficiency of 80%, TbL1\_4 is an interesting candidate material for a new green phosphor in LEDs.

## 4.6 References

- [1] R. Haitz and J.Y. Tsao, *Optik & Photonik*, 6 (2011) 26-30.
- [2] E.F. Schubert, J.K. Kim, H. Luo, and J.Q. Xi, *Rep. Prog. Phys.*, 69 (2006) 3069-3099.
- [3] C.C. Lin and R.-S. Liu, *J. Phys. Chem. Lett.*, 2 (2011) 1268-1277.
- [4] A.A. Setlur, *Electrochem. Soc. Interface*, 18 (2009) 32-36.
- [5] S. Ye, F. Xiao, Y.X. Pan, Y.Y. Ma, and Q.Y. Zhang, *Mater. Sci. Eng., R*, 71 (2010) 1-34.
- [6] H.A. Höpfe, *Angew. Chem., Int. Ed.*, 48 (2009) 3572-3582.
- [7] M. Raukas, J. Kelso, Y. Zheng, K. Bergenek, D. Eisert, A. Linkov, and F. Jermann, *J. Solid State Sci. Technol.*, 2 (2013) R3168-R3176.
- [8] K. Binnemans, *Chem. Rev.*, 109 (2009) 4283-4374.
- [9] K. Binnemans, *Rare earth beta-diketonates*, in *Handbook on the Physics and Chemistry of Rare Earths*, 2005, Elsevier. 107-272.
- [10] M.L.P. Reddy, V. Divya, and R.O. Freire, *Dalton Trans.*, 40 (2011) 3257-3268.
- [11] T.J. Mooibroek, P. Gamez, A. Pevec, M. Kasunič, B. Kozlevčar, W.T. Fu, and J. Reedijk, *Dalton Trans.*, 39 (2010) 6483-6487.
- [12] K.P. Zhuravlev, V.I. Tsaryuk, I.S. Pekareva, J. Sokolnicki, and Z.S. Klemenkova, *J. Photochem. Photobiol., A*, 219 (2011) 139-147.
- [13] K. Zhuravlev, V. Tsaryuk, J. Legendziewicz, V. Kudryashova, P. Gawryszewska, and V. Zolin, *Opt. Mater.*, 31 (2009) 1822-1824.
- [14] K. Manseki and S. Yanagida, *Chem. Commun.*, (2007) 1242-1244.
- [15] M. Latva, H. Takalo, V.M. Mikkala, C. Matachescu, J.C. Rodriguez-Ubis, and J. Kankare, *J. Lumin.*, 75 (1997) 149-169.
- [16] Z. Pan, G. Jia, C.-K. Duan, W.-Y. Wong, W.-T. Wong, and P.A. Tanner, *Eur. J. Inorg. Chem.*, 2011 (2011) 637-646.
- [17] N.M. Shavaleev, R. Scopelliti, F. Gumy, and J.-Claude G. Bünzli, *Inorg. Chem.*, 48 (2009) 6178-6191.
- [18] V. Tsaryuk, K. Zhuravlev, V. Zolin, P. Gawryszewska, J. Legendziewicz, V. Kudryashova, and I. Pekareva, *J. Photochem. Photobiol., A*, 177 (2006) 314-323.
- [19] J.C. de Mello, H.F. Wittmann, and R.H. Friend, *Adv. Mater.*, 9 (1997) 230-232.
- [20] T. Kottke and D. Stalke, *J. Appl. Crystallogr.*, 26 (1993) 615-619.
- [21] G.M. Sheldrick, *Acta Crystallogr., Sect. A: Found. Crystallogr.*, 64 (2008) 112-122.
- [22] G.M. Sheldrick, *SHELXS-97*, Bruker AXS Inc., Madison, Wisconsin, 1997.
- [23] Nonius, *COLLECT*, Nonius BV, Delft, The Netherlands, 2002.
- [24] L. Farrugia, *J. Appl. Crystallogr.*, 32 (1999) 837-838.
- [25] H.R. Hoveyda, V. Karunaratne, S.J. Rettig, and C. Orvig, *Inorg. Chem.*, 31 (1992) 5408-5416.

- [26] A. Minkkilä, M.J. Myllymäki, S.M. Saario, J.A. Castillo-Melendez, A.M.P. Koskinen, C.J. Fowler, J. Leppänen, and T. Nevalainen, *Eur. J. Med. Chem.*, 44 (2009) 2994-3008.
- [27] A.G. Orpen, L. Brammer, F.H. Allen, O. Kennard, D.G. Watson, and R. Taylor, *J. Chem. Soc., Dalton Trans.*, (1989) S1-S83.
- [28] W.T. Carnall, P.R. Fields, and K. Rajnak, *J. Chem. Phys.*, 49 (1968) 4450-4455.
- [29] W.T. Carnall, P.R. Fields, and K. Rajnak, *J. Chem. Phys.*, 49 (1968) 4447-4449.
- [30] L. Zhang, Y. Ji, X. Xu, Z. Liu, and J. Tang, *J. Lumin.*, 132 (2012) 1906-1909.
- [31] U. Baisch, D.B. Dell'Amico, F. Calderazzo, R. Conti, L. Labella, F. Marchetti, and E.A. Quadrelli, *Inorg. Chim. Acta*, 357 (2004) 1538-1548.
- [32] Q. Yu, X. Zhou, M. Liu, J. Chen, Z. Zhou, X. Yin, and Y. Cai, *J. Rare Earth.*, 26 (2008) 178-184.
- [33] X. Qiu, Y. Zhang, and X. Li, *J. Rare Earth.*, 27 (2009) 797-800.
- [34] S. Liu, L. Gelmini, S.J. Rettig, R.C. Thompson, and C. Orvig, *J. Am. Chem. Soc.*, 114 (1992) 6081-6087.
- [35] Z. Wang, J. Reibenspies, and A.E. Martell, *Inorg. Chem.*, 36 (1997) 629-636.
- [36] M. Nishio, *CrystEngComm*, 6 (2004) 130-158.
- [37] P. Bag, S. Dutta, P. Biswas, S.K. Maji, U. Florke, and K. Nag, *Dalton Trans.*, 41 (2012) 3414-3423.
- [38] G. Bombieri, F. Benetollo, A. Polo, K.K. Fonda, and L.M. Vallarino, *Polyhedron*, 10 (1991) 1385-1394.
- [39] S. Fleming, C.D. Gutsche, J.M. Harrowfield, M.I. Ogden, B.W. Skelton, D.F. Stewart, and A.H. White, *Dalton Trans.*, (2003) 3319-3327.
- [40] S.K. Langley, B. Moubaraki, and K.S. Murray, *Inorg. Chem.*, 51 (2012) 3947-3949.
- [41] G.B. Deacon, C.M. Forsyth, P.C. Junk, and A. Urbatsch, *Eur. J. Inorg. Chem.*, 2010 (2010) 2787-2797.
- [42] K. Xiong, X. Wang, F. Jiang, Y. Gai, W. Xu, K. Su, X. Li, D. Yuan, and M. Hong, *Chem. Commun.*, 48 (2012) 7456-7458.
- [43] L. Huang, L. Han, D. Zhu, L. Chen, and Y. Xu, *Inorg. Chem. Commun.*, 21 (2012) 80-83.
- [44] S. Romero, A. Mosset, and J.C. Trombe, *J. Solid State Chem.*, 127 (1996) 256-266.
- [45] C. Serre, J. Marrot, and G. Férey, *Inorg. Chem.*, 44 (2005) 654-657.
- [46] R. Reisfeld, E. Zigansky, and M. Gaft, *Mol. Phys.*, 102 (2004) 1319 - 1330.
- [47] B. Francis, D.B.A. Raj, and M.L.P. Reddy, *Dalton Trans.*, 39 (2010) 8084-8092.
- [48] R.J. Wiglusz, T. Grzyb, A. Lukowiak, P. Głuchowski, S. Lis, and W. Strek, *Opt. Mater.*, 35 (2012) 130-135.
- [49] L. Armelao, S. Quici, F. Barigelletti, G. Accorsi, G. Bottaro, M. Cavazzini, and E. Tondello, *Coord. Chem. Rev.*, 254 (2010) 487-505.
- [50] J.-C.G. Bünzli, *Chem. Rev.*, 110 (2010) 2729-2755.
- [51] M.H.V. Werts, R.T.F. Jukes, and J.W. Verhoeven, *Phys. Chem. Chem. Phys.*, 4 (2002) 1542-1548.
- [52] J.W. Verhoeven, *Pure Appl. Chem.*, 68 (1996) 2223-2286.
- [53] S. Petoud, J.-C.G. Bünzli, T. Glanzman, C. Piguet, Q. Xiang, and R.P. Thummel, *J. Lumin.*, 82 (1999) 69-79.
- [54] W.M. Faustino, O.L. Malta, and G.F. de Sa, *J. Chem. Phys.*, 122 (2005) 054109.

- [55] V. Tsaryuk, K. Zhuravlev, V. Kudryashova, V. Zolin, J. Legendziewicz, I. Pekareva, and P. Gawryszewska, *J. Photochem. Photobiol., A*, 197 (2008) 190-196.
- [56] G. Blasse, *Mater. Chem. Phys.*, 16 (1987) 201-236.
- [57] G.K. Liu, M.P. Jensen, and P.M. Almond, *J. Phys. Chem. A*, 110 (2006) 2081-2088.
- [58] L. Benisvy, P. Gamez, W.T. Fu, H. Kooijman, A.L. Spek, A. Meijerink, and J. Reedijk, *Dalton Trans.*, (2008) 3147-3149.
- [59] C. Li and M.Z. Hoffman, *J. Phys. Chem. B*, 103 (1999) 6653-6656.
- [60] V. Tsaryuk, K. Zhuravlev, V. Kudryashova, V. Zolin, Y. Yakovlev, and J. Legendziewicz, *Spectrochim. Acta A*, 72 (2009) 1020-1025.